

This is the peer reviewed version of the following article:

A combined numerical approach for the thermal analysis of a piston water pump / Milani, M.; Montorsi, L.; Venturelli, M.. - In: INTERNATIONAL JOURNAL OF THERMOFLUIDS. - ISSN 2666-2027. - 7-8:(2020), pp. 100050-100060. [10.1016/j.ijft.2020.100050]

Terms of use:

The terms and conditions for the reuse of this version of the manuscript are specified in the publishing policy. For all terms of use and more information see the publisher's website.

19/12/2025 01:07

A COMBINED NUMERICAL APPROACH FOR THE THERMAL ANALYSIS OF A PISTON WATER PUMP

M. Milani, L. Montorsi, M. Venturelli

DISMI – University of Modena and Reggio Emilia Via Amendola 2 – Padiglione
Morselli, 42122 Reggio Emilia, Italy

ABSTRACT

The paper proposes a numerical model for the investigation of a piston water pump under different operating conditions. In particular, the lubricating system is analysed and modelled. The study accounts for the lubrication and friction phenomena, heat transfer, multiphase fluid approach and motion simulation.

A computational thermo fluid dynamics approach has been adopted to develop a numerical tool able to simulate the behaviour of the oil during the machine working phases. The CFD approach simulates the moving metal components by means of moving meshes techniques; the friction phenomenon is estimated on the basis of formulations available in literature. The numerical model evaluates the heat transfer between moving metal parts and oil during the operating phases of the system. Furthermore, the heat transfer between oil and environment is calculated, accounting for conduction through the metal crankcase walls. A multiphase fluid approach is used for the simulation of the oil and air mixing during the crank rotation.

The heat transfer coefficient predicted by the CFD approach are employed in a lumped and distributed numerical model; the reliability and accuracy of the proposed numerical approach is addressed and validated against experimental results. Experimental data have been collected by means of a thermographic camera and thermocouples. Finally, the tool's predictive capabilities are addressed by simulating different working conditions.

KEYWORDS: heat transfer, friction, piston water pump, CFD, lumped parameter, moving mesh.

1. INTRODUCTION

Water piston pumps are largely employed in many industrial applications, but they are mainly used in the urban sector, fitted on drain cleaning trucks, waste bin washers and road sweepers. Bigger size pumps are used for ship keels cleaning. Due to the machine versatility, the pump can operate continuously or not; in addition, it can be used in cold country as well as in hot places. Thus, it is fundamental to project the machine in order to ensure the necessary heat transfer from the internal moving parts to the external environment. Therefore, overheating must be avoided to guarantee the performance and the lifetime of the pump itself for each working condition. A key role is played by lubricant oil which is the transfer fluid that transmit the heat from cranks, rods, pistons and crankshaft to the crankcase walls.

A great support can be offered to engineers by numerical simulations, in order to predict heat transfer for different working conditions of many systems and components. In particular, computational fluid dynamics models are largely employed to describe the thermo fluid dynamics behaviour of various machines. Bhutta et al. [1] presented a complete review of CFD analysis of heat exchangers. Different turbulence models and

velocity-pressure coupling schemes have been compared, for a wide variety of heat exchanger architectures. In this regard, H. Mroue et al. [2] investigated the performance of a heat exchanger equipped with six thermosyphons by means of a CFD approach without simulating the two-phase change that occurs inside the thermosyphons; an overview of numerical models used to investigate the condensation, evaporation and boiling in these systems can be found in [3].

Within the context of centrifugal pumps, a critical review of different CFD models has been presented by Shah et al. [4] in order to outline the most interesting areas of research to improve the pump performance: cavitation analysis, diffuser pump analysis, volute flow study and impeller-volute interaction.

In order to simulate the thermo fluid dynamics behaviour of the oil inside the crankcase, different phenomena must be accounted for. Firstly, attention should be devoted to the movement description of cranks, rods, pistons, and crankshaft that caused the oil-air mixing (splash lubrication). Moving meshes give the possibility to the user to include moving parts, based on equations well known in literature [5, 6]. This numerical technique is expensive in terms of computational resources, but it ensures good accuracy in modelling moving parts and solid fluid moving interfaces. Menéndez Blanco and Fernández Oro [7], for instance, used this numerical approach to construct a model of an air-operated piston pump for lubricating greases. Subsequently, it is necessary to calculate the thermal energy introduced into the system by friction. Different approaches can be found in literature [5, 6, 8, 9, 10, 11], referred to analysis of engine pistons. Indeed, piston water pumps and engines present similar architectures of pistons, crank mechanisms, rings. In particular, detailed descriptions of the friction between the piston rings and the cylinder wall have been outlined by Cho and Moon [6] and by Livanos and Kyrtatos [8], while Tateishi [9] proposed an empirical approximation. One of the most applied equation in numerical modelling is the Chen and Flynn correlation [10], used also by Hooper et al. [11] to successfully simulate a stepped piston engine using one dimensional CFD approach. Once calculated the heat released by friction, fluid properties and heat transfer models must be defined. The fluid is described as a two phases mixture of air and oil; thus, the volume of fluid (VOF) approach is used. Several examples of VOF simulations are available in literature applied to different contexts. Jouhara et al. [12] simulated flow and heat transfer in a thermosyphon: by means of VOF technique, evaporation and condensation were accounted for as well as the interaction between gas and liquid. Lückmann et al. [13] applied the numerical method to resolve the free-surface oil flow in a lubricant oil pumping system of a reciprocating compressor.

In [14] a numerical approach has been used to predict the transient behaviour of a lubrication in a wet clutch of a hydromechanical variable transmission; the volume of fluid approach has been employed in the numerical model in order to determine the oil distribution in the clutch region under different rotating velocities. A similar study was conducted by Terzi et al [15] where a VOF approach has been used to determine the lubrication flow within a multi-plate wet clutch.

Air and oil physical properties need to be updated on the basis of the temperature field: while air property correlations are included in the library of the software, oil ones have to be provided. Habchi et al. [16] developed and validated models of pressure and temperature dependencies of standard oil properties. Heat transfer problems have been widely simulated by means of numerical models, especially for heat exchangers [1]. Also heat transfer in cylinder walls has been largely studied: Rakopoulos et al. [17]

compared different heat transfer formulations. In this paper, dimensionless numbers [18, 19] are involved in correlations [20, 21] able to described the heat transfer coefficient in a very simple way. Brucker and Majdalani [20] presented a comprehensive table of Nusselt number expressions for different geometries, flow conditions and ranges of validity. In particular, the equation proposed by Churchill and Chu [21] is used to calculate the Nusselt number that characterized the heat transfer between the crankcase walls and the environment. A similar approach has been successfully used by Bottazzi et al. [22] to construct and to develop a numerical model able to simulate the thermodynamics behaviour of a coffee roasting machine and, in particular, the heat transfer from a hot air flow to coffee beans during toasting phases.

The aim of this study is the development of a numerical tool that can be used for the investigation of lubricating system for piston water pump in order to design new crankcase and to improve existing components.

Thus, the model is intended to predict the influence of the various parameters that characterize the heat transfer between oil and metal parts, such as surface geometry, temperature and oil mixing. The main goal of the numerical tool is to predict the evolution of the temperature map in order to define the steady value for different working conditions.

Finally, the accuracy of the numerical results of the proposed model are validated against experimental data. The experimental measurements+ are collected by means of thermocouples and a thermographic camera applied to a standard pump tested for different working conditions.

2. CFD MODEL

Piston water pump are generally composed of three alternative pistons, with 120° of angular displacement between each one. A complete numerical model of the pump can be obtained joining three single models representing one piston. Thus, initially, a single model regarding a crank, a rod and a piston is developed. Once prepared the geometry, the mesh is constructed. As previously said, moving mesh technique is applied in order to simulate the splash lubrication effects. Motion of each moving part need to be modelled. Thus, energy dissipated due to the friction is estimated and introduced into the system. For fluid modelling, a “Volume of Fluid” approach is used, in order to describe the two phases mixture of oil and air. Oil properties are expressed as a function of the temperature. Finally, heat transfer from metal moving part to the environment is defined by means of dimensionless formulations. The implementation of all these features is necessary in order to ensure a good accuracy of the model, but it determines a high computational effort. In addition, the heat transfer phenomenon is a slow mechanism that requires a long computational time. Thus, a 2D model is used in order to obtain a model that can be usefully adopted by pump designers: indeed, the model accuracy is important as well as the possibility to obtain the results in a reasonable time. Once all the features are properly configured in the 3D single piston model, it is possible to automatically scale from the 3D to a 2D model using a section plane that includes the axis of the central piston and that is perpendicular to the pump base.

2.1 Motion model

The single piston model accounts for two moving parts: the rod and the piston. Both the motions of the rod and the piston are simulated by means of moving mesh technique. In

the first case, two blocks are constructed: a fixed one, that is the void of the crankcase, and a moving one that accounts for the rod. Indeed, this last one is a box that includes the rod and that moves inside the fixed block. This movement is the rod motion and it is possible to define it with a geometrical analysis [5]. Referring to the layout of Fig. 1, rod position on a plane XY is described by Eq. 1 and Eq. 2:

$$x_B = r_c \cdot \cos(\omega \cdot t - \pi) \quad (1)$$

$$y_B = r_c \cdot \sin(\omega \cdot t - \pi)$$

(2)

where x and y are the position coordinates of the point B referred to the fixed system shown in Fig. 1; r_c is the eccentricity, i.e. the crank length, ω is the rotational velocity, t is the time, $-\pi$ is summed because the simulation starts when the piston is at the bottom dead centre (BDC). A roto-translation of rigid body is defined when the motion of a generic point J (Eq. 3) is known. Considering the generic point J , its movement respect the fixed coordinate system can be described as the vectorial sum of the translation velocity of a moving system and the rotational velocity referred to that system. The moving coordinate system is constructed with axes parallel to the ones of the fixed system and origin in B . The rotational axis coincides to the Y axis of the moving system.

$$\vec{v}_{totJ} = \vec{v}_{transB} + \vec{\beta}_B \times \overline{BJ} \quad (3)$$

The components of the translational velocity of the moving system are expressed by Eq. 4 and Eq. 5, while the angular velocity is calculated with Eq. 6.

$$\dot{x}_B = -\omega \cdot r_c \cdot \sin(\omega \cdot t - \pi) \quad (4)$$

$$\dot{y}_B = \omega \cdot r_c \cdot \cos(\omega \cdot t - \pi) \quad (5)$$

$$\dot{\beta}_B = \lambda \cdot \omega \cdot \left(\frac{\cos(\omega \cdot t)}{\sqrt{1 - \lambda^2 \cdot \sin^2(\omega \cdot t)}} \right) \quad (6)$$

Deriving Eq. 1 and Eq. 2 respect time, it is possible obtain Eq. 3 and Eq. 4. With simple mathematical steps (see Appendix A) it is possible to determine Eq. 6, where λ is the ratio between crank and rod length. The software automatically applies Eq. 3 to all the cells of the moving mesh, once introduced Eq. 4 and Eq. 5 and Eq. 6.

Once the rod movement is detailed, piston motion is simulated. To do that, a second overset mesh is configured. As done for the rod, the void of the crankcase is used as fixed block, while a moving block accounts for the piston. The motion is a translation of a rigid body and it can be described on the basis of the motion equation of the small end connecting rod (point A in Fig. 1) obtained from the analysis of a generic crank-rod mechanism (see Appendix A).

$$\dot{x}_A = r_c \cdot \omega \cdot \left[\sin \alpha + \frac{\lambda \cdot \sin 2\alpha}{2 \cdot \sqrt{1 - \lambda^2 \cdot \sin^2 \alpha}} \right] \quad (7)$$

The two moving blocks of the overset mesh zones are overlapping each other; thus, a third overset interface has to be configured in order to assign the correct behaviour to each cell that are positioned in the overlapping region between rod and piston blocks.

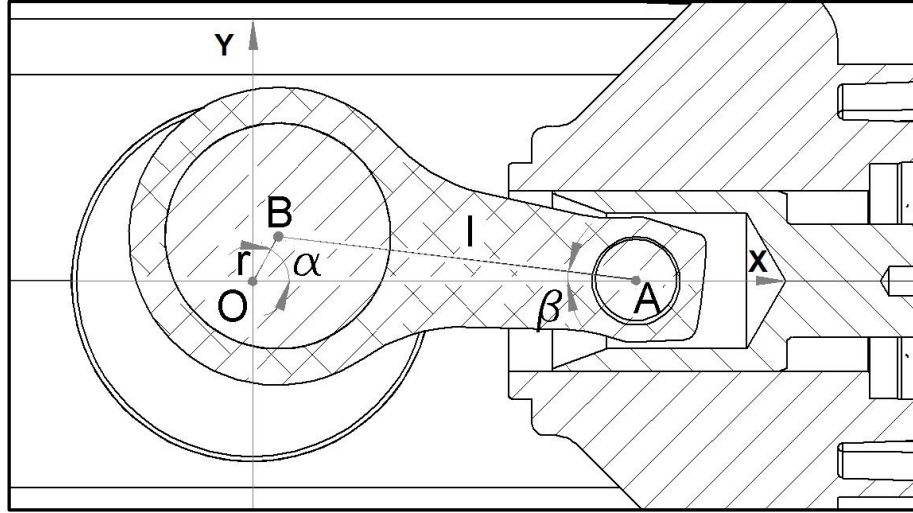


Fig. 1. Crank-rod mechanism, reference system.

Friction analysis has a key role to assess the dissipated energy. It is very useful to assess at each contact surface the amount of energy that is released as heat. Unfortunately, no studies are available in literature that investigate friction evaluation on a piston water pump. On the contrary, there are some interesting works accounting for friction on an internal combustion engine [5, 6, 8, 9, 10, 11]. Water piston pumps and engines presented a quite similar architecture, in terms of crank-connecting rod mechanism, piston and rings. Dissipated energy due to friction in an engine, is frequently calculated as a whole, on the basis of energy balance, but in a few cases it is possible to found approximated correlation regarding the various contact surfaces.

According to Heywood [5], Eq. 8 can be used to calculate the friction force F_{f_rbe} referred to the contact between the connecting rod big end and the crankshaft, under the hypothesis of continuous oil film between the surfaces:

$$F_{f_rbe} \approx (\pi \cdot d_{rbe} \cdot l_{rbe}) \cdot \mu_{oil} \cdot \left(\frac{\pi \cdot d_{rbe} \cdot \omega}{\bar{c}_{rbe}} \right) = \frac{\mu_{oil} \cdot \pi^2 \cdot d_{rbe}^2 \cdot l_{rbe} \cdot \omega}{\bar{c}_{rbe}} \quad (8)$$

Where d_{rbe} is the internal diameter of the connecting rod big end, l_{rbe} is the contact length (thickness of connecting rod big end), μ_{oil} is the oil dynamics viscosity, \bar{c}_{rbe} is the mean radial clearance. Once obtained the friction force by means of this approximated approach, it is possible to determine the related friction torque M_{f_rbe} (Eq. 9) and the dissipated power P_{f_rbe} (Eq. 10):

$$M_{f_rbe} = F_{f_rbe} \cdot d_{rbe} / 2 \quad (9)$$

$$P_{f_rbe} = M_{f_rbe} \cdot \omega \quad (10)$$

The same approach can be applied to assess the dissipated power P_{f_rse} referred to the contact surface between the connecting rod small end and the pin. This contact, in fact, presents a similar geometry configuration (cylinder vs. cylinder contact surface) and an analogous lubrication condition. Another important contribution to the energy dissipation is the friction between the crankshaft and the two needle bearings. An approximated method to choose size the component is provided by producers. Each needle bearing supports a force F_{f_nb} :

$$F_{f_nb} = p_{\max} \cdot (\pi \cdot d_p^2 / 4) \cdot n_p / 2 \quad (11)$$

where p_{\max} is the water maximum pressure, d_p the piston diameter, n_p the number of pistons. Obviously, the force is divided by two because there are two needle bearings. The related friction torque M_{f_nb} can be calculated by means of Eq.12:

$$M_{f_nb} = 0.5 \cdot C_f \cdot d_{nb} \cdot F_{f_nb} \quad (12)$$

where C_f is the constant friction coefficient, value characteristic of the bearing architecture and tabulated by the producers, d_{bn} is the internal diameter of the component (where the crankshaft is connected). Thus, the related dissipated power can be assessed by Eq. 10.

In order to complete the friction evaluation, two additional dissipated power terms have to be accounted for: the first one is due to the contact surface between the seal placed in the cylinder wall and the ceramic piston part (P_{f_ring}) and the second one is referred to the friction between the journal box and the piston (P_{f_jb}). To calculate these two terms, several approaches referred to engine pistons are available in literature [8, 9] but in this case to consider the piston water pump as an engine is a poor approximation, due to the different ring kind and number for each piston and due to the different pressure curve during the cycle. A different approach can be based on efficiency analysis. The ratio between hydraulic (P_{hyd}) and mechanical (P_{mech}) power is the total efficiency of the pump η_{tot} :

$$\eta_{tot} = \frac{P_{hyd}}{P_{mech}} = \frac{Q \cdot (p_{\max} - p_{suc})}{\omega \cdot M_{\max}} = \eta_{vol} \cdot \eta_{hm} \quad (13)$$

where Q is the flow rate, p_{suc} the pressure at the pump suction and M_{\max} the maximum torque, referred to the maximum pressure p_{\max} . The total efficiency η_{tot} is equal to the product of volumetric efficiency η_{vol} and hydromechanical efficiency η_{hm} :

$$\eta_{vol} = Q / [3 \cdot \omega \cdot (2 \cdot r_c) \cdot (\pi \cdot d_p^2 / 4)] \quad (14)$$

while η_{vol} is defined as the ratio between the flow rate and the ideal geometrical flow rate, η_{hm} can be obtained on the basis of experimental data combining Eq. 14 with Eq. 13. The total dissipated power P_{f_tot} can be calculated as:

$$P_{f_tot} = P_{hyd} \cdot (1 - \eta_{hm}) = 2 \cdot P_{f_nb} + 3 \cdot (P_{f_rbe} + P_{f_rse} + P_{f_jb} + P_{f_ring}) \quad (15)$$

afterwards, subtracting the previously calculated terms of dissipated power, it is possible to estimate the sum of the two investigated terms. Based on producer's know-how, the ratio between the terms is fixed: thus, P_{f_ring} and P_{f_jb} can be separately assessed.

The total friction losses on the piston is calculated by both the proposed approach and the Chen and Flynn correlation [10] and the results are compared as a check. This empirical correlation is one of most used technique to estimate the total dissipated power due to the friction in combustion chamber simulation. Both the approaches provide results of the same order.

In the constructed model, the dissipated power terms are included as thermal flux from the contact surface to the fluid. The rod is made of aluminium, that is a good conductor; thus, the hypothesis of uniform energy distribution can be assumed and both P_{f_rbe} and P_{f_rse} are addressed to the external rod surface. A uniform energy distribution is also

supposed assigning P_{f_jb} to the part of the cylinder internal wall that is immersed in oil. P_{f_ring} is referred to the cylinder and the piston parts those work in contact with water and do not influence the oil behaviour: thus, P_{f_ring} is not included in the numerical model. P_{f_nb} , instead, must be accounted for in the overall numerical model of the pump but not in the single piston model.

2.3 Fluid model

The fluid inside the crankcase is modelled as a multiphase non reacting mixture by means of the Volume of Fluid approach. The spatial distribution of each phase at a given time is defined in terms of volume fraction. The Segregated Flow model is used to solve the conservation equations separated for each phase, except for the pressure field which is common. In this study, also the temperature field has to be accounted for; the model used is the Segregated Multi-Phase Temperature.

The two phases considered are air and lubricant oil. While the air physical properties are included in the software data base as temperature and pressure dependant, the oil ones must be provided by the user. The temperature influence on density and viscosity at atmospheric pressure can be obtained from the oil data sheet. In order to define the heat transfer, also oil thermal properties have been detailed. Brucker and Majdalani [20] proposed empirical correlations pressure and temperature dependant to calculate specific heat c_{poil} and thermal conductivity k_{oil} of an oil similar to the one used in the piston water pump.

$$k_{oil} = C_0 + C_1 \cdot \left\{ \left(V_{oil} / V_{oil_ref} \right) \cdot \left[1 - 0.101 \cdot \left(T_{oil} / T_{oil_ref} \right) \cdot \left(V_{oil} / V_{oil_ref} \right)^3 \right] \right\}^{-7.6} \quad (16)$$

$$c_{p_{oil}} = \left[C_2 + C_3 \cdot \left(T_{oil} / T_{oil_ref} \right) \cdot \left(V_{oil} / V_{oil_ref} \right)^4 \right] / \rho_{oil} \quad (17)$$

The oil volume and temperature at actual conditions are V_{oil} and T_{oil} while V_{oil_ref} and T_{oil_ref} are related to reference values; C_0 , C_1 , C_2 and C_3 are empirical coefficients and ρ_{oil} is the oil density. During the working condition of the pump, the oil in the crankcase is constantly at atmospheric pressure; thus, the two equation can be simplified because the V_{oil} / V_{oil_ref} ratio is equal to 1. In fact, the pump has a breather plug and the model accounts for it by means of an air inlet at the atmospheric pressure (see Fig. 2). Thus, only air can enter the crankcase but both oil and air can exit. In particular, a very small amount of oil can exit from the breather plug, if it is thrown to the plug by the moving rod. All the other surfaces are considered as “wall” (no mass transfer is allowed by the boundaries between internal crankcase and the environment).

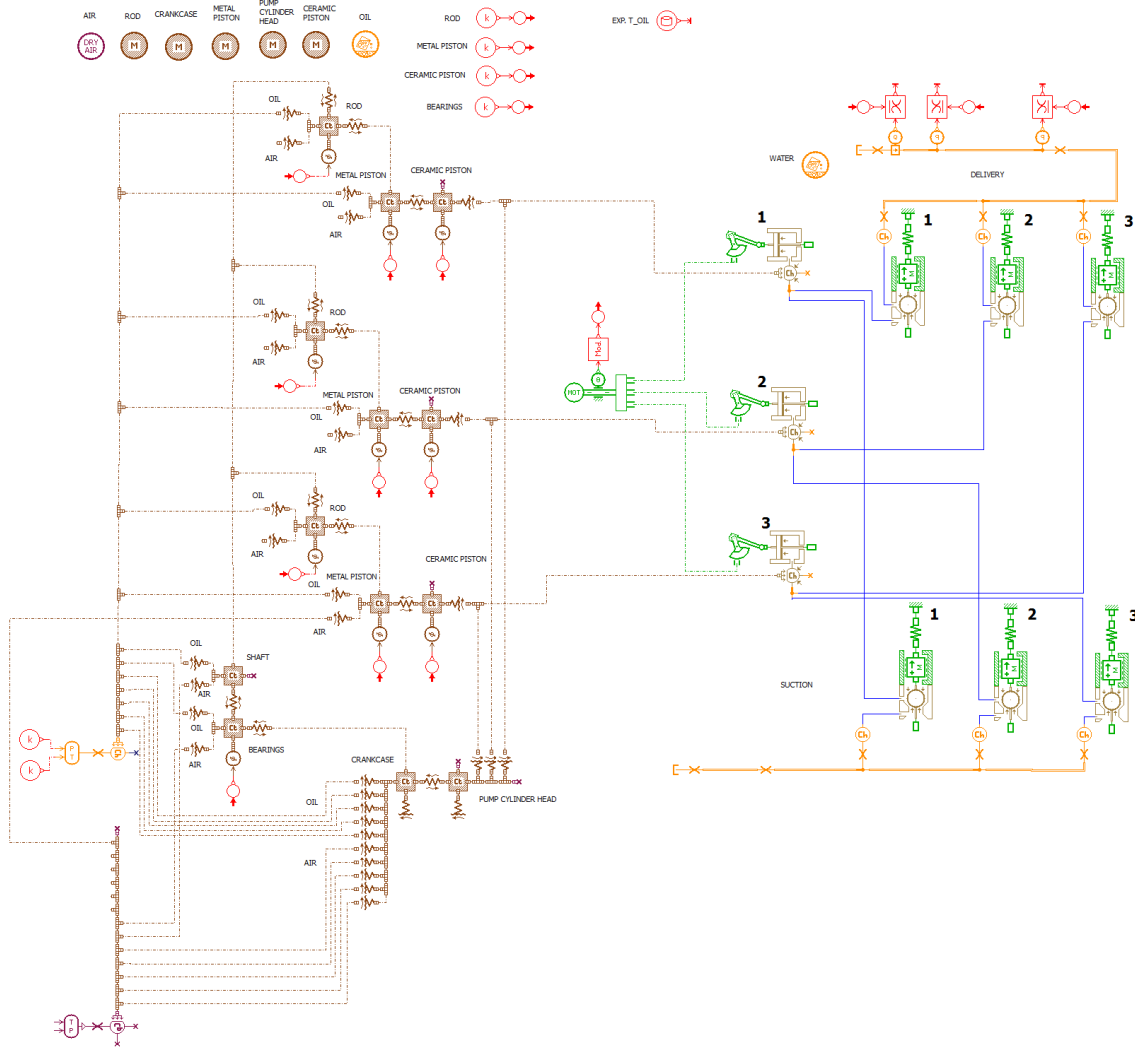


Fig. 2. Lumped parameter model, layout of the whole pump

2.4 Heat transfer model

Once calculated the dissipated power due to friction and modelled the two-phases fluid mixture, heat transfer must be defined. From the surfaces interested by power dissipation, the heat is transferred to the fluid. Heat transfer between the two phases are automatically included, as well as convection between the fluid and the crankcase internal walls. In order to account for the thermal power transferred (W_{cond}) through the walls due to the conduction phenomenon, Eq. 18 is used: T_{wall_int} and T_{wall_ext} are, respectively, the internal and external wall temperature, S_{wall_int} is the heat transfer surface and R_{wall} the wall thermal resistance.

$$W_{cond} = (T_{wall_int} - T_{wall_ext}) \cdot S_{wall_int} / R_{wall} = (T_{wall_int} - T_{wall_ext}) \cdot S_{wall_int} / (s_{wall} / k_{wall}) \quad (18)$$

The wall thermal resistance R_{wall} has been evaluated based on the wall thickness s_{wall} and the thermal conductivity k_{wall} of the metal. Afterwards, the thermal power W_{conv} is dissipated towards the environment (natural convection) and it can be calculated as proposed in Eq. 19.

$$W_{conv} = (T_{wall_ext} - T_{env}) \cdot S_{wall_ext} \cdot h_{wall_ext} \quad (19)$$

The environment is at atmospheric pressure and its temperature is T_{env} , the transfer surface is the external area S_{wall_ext} of the crankcase and h_{wall_ext} is the heat transfer coefficient. In order to define this parameter, a non-dimensional approach is used. It is possible to evaluate the Nusselt number Nu_{wall_ext} as a function of the Reynolds number Re_{wall_ext} and of the environment Prantl number Pr_{env} (see Apeendix B). Once obtained Nu_{wall_ext} , the heat transfer coefficient can be calculated according to Eq. 20, where l_{wall_ext} is a characteristic length of the transfer surface and k_{env} is the thermal conductivity of the environment.

$$Nu_{wall_ext} = (h_{wall_ext} \cdot l_{wall_ext}) / k_{env} = f(Re_{wall_ext}, Pr_{env}) \quad (20)$$

The connecting function must be chosen based on the transfer surface shape, the flow conditions, the validity range of the non-dimensional numbers. Brucker and Majdalani [20] shown a comprehensive table of Nusselt number correlations for all these parameters. Equation 21 had been proposed by Churchill and Chu [21] and it was developed for natural convection from a planar surface and for $10^0 < Ra < 10^9$.

$$Nu_{wall_ext} = 0.68 + \frac{0.67 \cdot Ra_{wall_ext}^{1/4}}{(1 + 0.67 \cdot Pr_{env}^{-9/16})^{4/9}} \quad (21)$$

where Ra_{wall_ext} is the Rayleigh number, obtained by multiplying the Grashof number, Gr_{wall_ext} , referred to the external crankcase surface and the Prandtl number, Pr_{env} , of the external ambient (see Appendix B). In order to calculate the Grashof number, the volumetric thermal expansion coefficient of the air b_{env} has to be taken into account:

$$b_{env} = -\frac{1}{\rho_{env}} \cdot \left(\frac{\partial \rho_{env}}{\partial T_{env}} \right)_p = \frac{1}{\rho_{env}} \cdot \frac{p_{env}}{Rg \cdot T_{env}^2} = \frac{1}{T_{env}} \quad (22)$$

As proposed by Incropera and DeWitt [18], the air can be considered as an ideal fluid for the evaluation of the volumetric thermal expansion coefficient; thus, it can be assumed to be equal to approximately $1/T$, where T is the absolute temperature of the gas (see Eq. 22).

3. LUMPED PARAMETER MODEL

In order to obtain a complete analysis of the overall machine, a lumped and distributed parameter model is constructed. Indeed, the developed 2D CFD model designed to describe the thermo-fluid dynamic behaviour of the lubricating system but is not applicable for a detailed study of the pump due to the high computational effort. In other words, an overall CFD model that includes both lubricating system and pumping zone, will cause an high computational resource request and long-time simulations; thus, a lumped and distributed parameter approach is the best compromise between computational effort and results' accuracy in order to develop a model that can be able to show the results in an admissible time and ensuring a good predictive capability.

As depicted by Fig. 2, the model of the pump is constructed connecting two main parts: the pumping side, where the operating fluid, water, is addressed by the piston chamber evolution from the suction to the delivery, and the mechanical side, where the lubricating system is placed. The model accounts for the thermo-dynamics behaviour of both sides; in particular, the heat transfer between the pump cylinder head and the

water, the crankcase and the pump cylinder head, the lubricating fluid and the crankcase, are included. There are parameters that can not be fixed on the basis of geometrical or physical information: in order to obtain these data, such as the convective heat transfer coefficient of each wall, the 2D CFD simulation is fundamental. On the other hand, the lubricating system simulation requires to fix the heat transferred from the crankcase to the pump cylinder head. Thus, the CFD lubricating system model and the lumped parameter model of the pump are deeply dependant each other and they need to be simultaneously developed.

3.1 Pumping side model

The piston chamber evolution of each of the three pistons, properly phased, is accounted for by this part of the model. Particular care is devoted to the modelling of the opening characteristic of the suction and delivery automatic valves by means of an accurate geometrical definition; in addition to this, the spring displacement –force relationship and the moving parts mass are also included. To complete the layout, the suction and delivery line are considered, as well as the tank at the atmospheric pressure value and an orifice used as pump load.

The hydraulic behaviour predicted by the model is tailored by means of experimental data, in terms of load pressure and flow rate and volumetric efficiency. The heat transfer between the pumping side and the mechanical side is permitted by means of the crankcase – pump cylinder head contact interface and by the ceramic piston part – metal piston part contact interface; these contact interfaces accounted for conduction, as well as convection phenomena. In fact, while the pump cylinder head and the ceramic piston part are cooled by the water flow, the crankcase and the metal piston part are in contact with the oil and they are hooted by the power dissipation due to the friction, as explained above. In addition, there is an amount of energy that is released as heat due to the friction between the ceramic piston part and the seal; this thermal power P_{f_ring} is included in the model and it is calculated by means of the approach described in the Paragraph 2.2.

In order to define the thermal power transferred by the pump cylinder head towards the environment, the heat transfer coefficient must be calculated. The numerical approach employed is the same used for the crankcase in the CFD model, based on the Nusselt number correlation of Eq. 21. As said above, the pump cylinder head is cooled by the water flow. The internal geometry of the component is really complex, but, as an approximation, it is possible to calculate the hydraulic diameter d_h and to consider the convection phenomenon as referred to a turbulent flow in circular tubes; in other words, the Nusselt number Nu_{head_int} is simulated by means of the Dittus-Boelter equation (as shown by Incropera and DeWitt [18]):

$$Nu_{head_int} = 0.023 \cdot Re_{head_int}^{4/5} \cdot Pr_{water}^{nc} \quad (23)$$

Where Re_{head_int} is the Reynolds number of the internal duct of the pump cylinder head, using the hydraulic diameter d_h as characteristic length l (see Appendix B), Pr_{env} is the water Prantl number and nc is a exponent equal to 0.4 for flow heating and 0.3 for flow cooling. Eq. 23 is normally used for small temperature difference and for the range of conditions: $0.6 \leq Pr \leq 160$, $Re \geq 10^4$, $l/d \geq 10$. Also the ceramic piston part is cooled by

water: the contact surface is a circular area that is moved inside the piston chamber. It is very difficult to define the flow condition. On the basis of the Reynolds number Re_{cer_p} , it is not possible to recognize a fully developed turbulent flow; thus, a correlation validated for mixed condition on a flat plate and for $0.6 \leq Pr \leq 60$, $5 \cdot 10^5 < Re < 10^8$, (Incropera and DeWitt [18]), can be used in order to obtain an average value of Nusselt number Nu_{cer_p} , and, consequently, an average value of heat transfer coefficient:

$$\overline{Nu}_{cer_p} = (0.037 \cdot Re_{cer_p}^{4/5} - 871) \cdot Pr_{water}^{1/3} \quad (24)$$

In the model, the conduction between two components is automatically calculated based on the material properties and the geometrical characteristic of the contact surface. In addition, it is possible to set a contact thermal resistance for cases where the surface roughness must be considered.

3.2 Mechanical side model

This part of the model focuses on the heat transferred between lubricating fluid and mechanical components by means of convection; the model includes also the conduction between the parts in contact. As mentioned above, each conduction interface requires the geometrical parameters and the involved material properties. The dissipation of mechanical power due to friction is considered by means of the approach described in the Paragraph 2.2 in the CFD model; more in details, P_{f_rbe} and P_{f_rse} are addressed to the rod as well as P_{f_jb} is referred to the metal piston part and P_{f_nb} , regards the needle bearings.

The lubricating fluid is composed of air and oil. The lumped parameter approach normally does not let the user to model a multiphase fluid; thus, two different virtual volumes (one of air and one of oil) are employed. The sum of the two volume is equal to the internal volume of the crankcase. Each volume can transfer heat with all the components that are in contact with the lubricating fluid, by means of various interfaces of area S_{eff} .

$$S_{eff} = nd \cdot S_{geo} \quad (25)$$

Where S_{geo} is the geometrical area and nd is a coefficient of covered area, obtained from the CFD simulation and equal to the surface average of the oil mass fraction (nd_{oil}) and the air mass fraction (nd_{air}). Thus, each contact interface is divided in two surfaces, one of area S_{eff_oil} referred to the oil and one of area S_{eff_air} referred to the air.

The thermal power transferred from the crankcase to the environment is described by means of the same approach (Eq. 21) used in the CFD model, while the heat transferred between the lubricating fluid (both air and oil) and each crankcase wall is modelled by means of the Eq. 24. Each wall of the crankcase is considered as a flat plat and is characterized by different geometry and oil/air distribution; the flow is described by a Reynolds number too low for a fully developed turbulent condition, thus, the Nusselt number correlation (Eq. 24) proposed seems to be a good approach to obtain the related heat transfer coefficient. In fact, air and oil are continually mixed inside the crankcase by the moving parts, but the fluid does not reach an average velocity sufficiently high to be in turbulent condition. For the same reason, also the Nusselt number referred to the

contact surface between the bearings and the lubricating fluid is calculated with the same approach (Eq. 24). The surface is the area between the bearing external circumference and the shaft external circumference. The heat transferred from the shaft to the lubricating fluid is accounted for by means of an approach validated for rotating cylinder in a cross flow (Incropera and DeWitt [18]):

$$\overline{Nu}_{sh_oil} = 0.193 \cdot Re_{sh_oil}^{0.618} \cdot Pr_{oil}^{1/3} \quad (26)$$

Where Re_{sh_oil} is the rotational Reynolds number of the oil dragged by that shaft (see Appendix B) and Pr_{oil} is the Prandtl number of the oil. This correlation is used for the range of conditions $0.7 \leq Pr$, $4 \cdot 10^3 \leq Re \leq 4 \cdot 10^4$ and it can be employed for both oil and air. For the contact surface between the rod and the lubricating fluid, the heat transfer coefficient is obtained by the 2D CFD simulation, as well as the one referred the interface between the metal piston part and the lubricating fluid. The 2D CFD model is also used, as said above, to calculate the coefficients of covered area for both oil and air, regarding all the considered contact surfaces.

4. CFD MODEL RESULTS

The results of the CFD model of the lubricating system in terms of heat transfer coefficient and oil and air distribution are then employed in the lumped and distributed numerical model.

In the CFD model, the rotational speed used is one thousand rpm and the employed time step is 0.1 millisecond; thus, angular time step is smaller than one degree. A breather plug is included in the geometry in order to maintain the atmospheric pressure of the fluid volume inside the crankcase. . Afterwards, the initial temperature value is set equal to the ambient temperature, while the initial oil and air distribution is shown in Fig. 3a. The oil mass fraction is equal to the 50% of the volume.

On the right side of the picture, a rectangular shape can be noticed that is a fictitious volume separated from the main volume by the piston. This volume is requested by the overset mesh technique in order to correctly describe the piston movement, but it is not referred to the real cylinder. In fact, in the real machine, on this side of the piston there is water, that is to say, the pumped fluid. This fictitious volume has the same initial pressure, temperature and air-oil distribution of the main volume but it is physically separated from the crankcase volume, thus, the air and oil in this region do not influence the fluid dynamic behaviour of the crankcase volume. In order to highlight this point, an open boundary is included in the simulation at the left side of the fictitious volume: after few crankshaft revolutions the volume is almost full of air at the environment conditions.

While the rod and the piston position at the BDC (bottom dead centre) are shown in the Fig. 3a and in the Fig. 3d, Fig. 3c depicts the machine in the TDC configuration (top dead centre) and an arbitrary angular position is chosen in Fig. 3b.

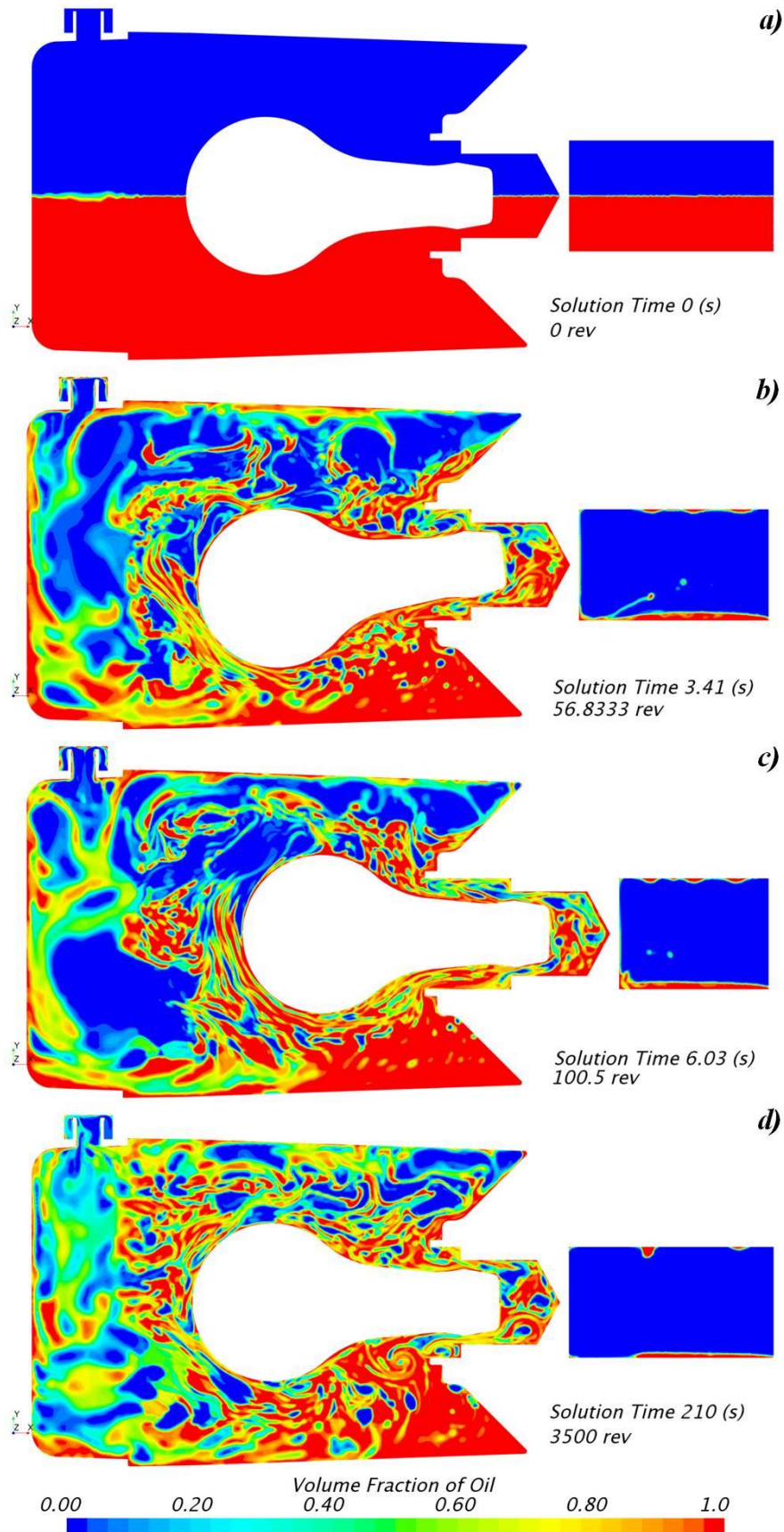


Figure 3- Volume fraction of oil in the crankcase, referred to a) initial condition; b) after 3.41 s c) after 6.03 s; d) after 210 s.

Fig. 3b displays the air-oil volume fraction after 3.4 seconds; the oil and air are mixed but a separation between the fluids can be still identified. A similar phenomenon can be noticed also in Fig. 3c, i.e. simulation time equal to 6 seconds which corresponds to 100 revolutions. The last picture, Fig. 3d, shows the oil volume fraction distribution when the system has reached a steady state condition, i.e. simulation time 210 s; the air and the oil are completely mixed.

In all the presented pictures, there is a no recirculating zone where oil is almost fixed, in the right-lower side, under the cylinder. A good oil recirculation is one of the most important goal for lubricating system design, so, if this behaviour will be confirmed also by the three-dimensional simulations, the crankcase geometry should be modified in order to avoid it. During the transient period, a small amount of oil can escape through the breather plug, as confirmed by experimental test, but after a few seconds these oil losses are no more observable. The oil amount in the fictitious volume, starting from the initial value, in a few revolutions decreased rapidly. Only a thin oil layer is still observable in the steady-state phase. As said above, this fictitious volume has no relation with the real cylinder, because the pumped fluid is water.

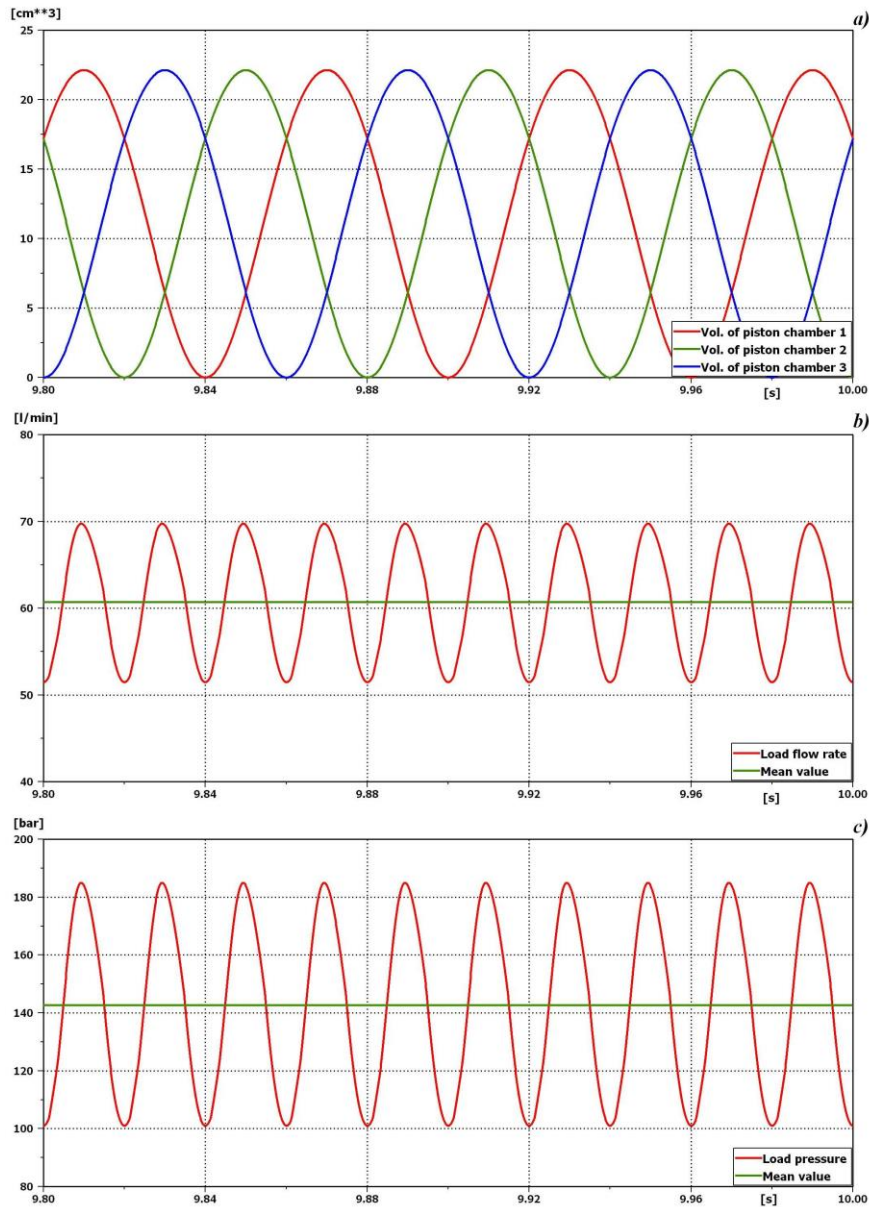
The results obtained from this 2D CFD model are compared to experimental measurements and a good agreement is obtained from a qualitatively point of view.

In fact, it is not possible to strictly compare the numerical data achieved from the 2D CFD model to the experimental data: converting from 3D to 2D, the crankcase walls parallel to the model plane are neglected. In other words, the crankcase area able to transfer heat from the fluid inside to the environment is different from the one of the real geometry. The thermal power introduced in the model due to friction is reduced to account for this consideration. In fact, the time duration of the numerical thermal transient is minor that the real one, but the numerical mean value of the oil temperature in steady-state condition is quite close to the experimental value.

Thus, the 2D model can not be used to predict exactly the punctual temperature evolution of the lubricating system but the qualitatively good agreement between numerical results and measurements lets the user to usefully employ the model to estimate the heat transfer coefficient and the air-oil distribution of each surface. These data are introduced in the lumped and distributed parameter model to obtain a predictive model of the pump. This approach, based on the use of a 2D CFD model and a lumped parameter model, has a computational effort minor than a complete 3D CFD model; thus, the combined approach demonstrated to be a reliable tool to achieve the numerical results with good accuracy.

5. LUMPED PARAMETER MODEL RESULTS

The lumped and distributed numerical model of the whole pump is tailored in two steps. Firstly, the pumping side is accounted in the analysis and the measurements are compared with the numerical results in terms of load pressure and flow rate. More in details, the discharge coefficient and the friction parameter of each valve are introduced and regulated in order to obtain a good agreement between numerical and experimental data. Particular care is devoted to the angular phasing of the three pistons: in Fig. 4a the volume evolution of the three piston chambers are shown. Figs. 4b and 4c depicts the instantaneous and the mean values of load pressure and flow rate. The curves are very close to the measurements; thus, the model is able to describe the fluid dynamics behaviour of the pumping side and it is possible to calculate the volumetric efficiency, that is equal to the experimental value and higher than 90%.



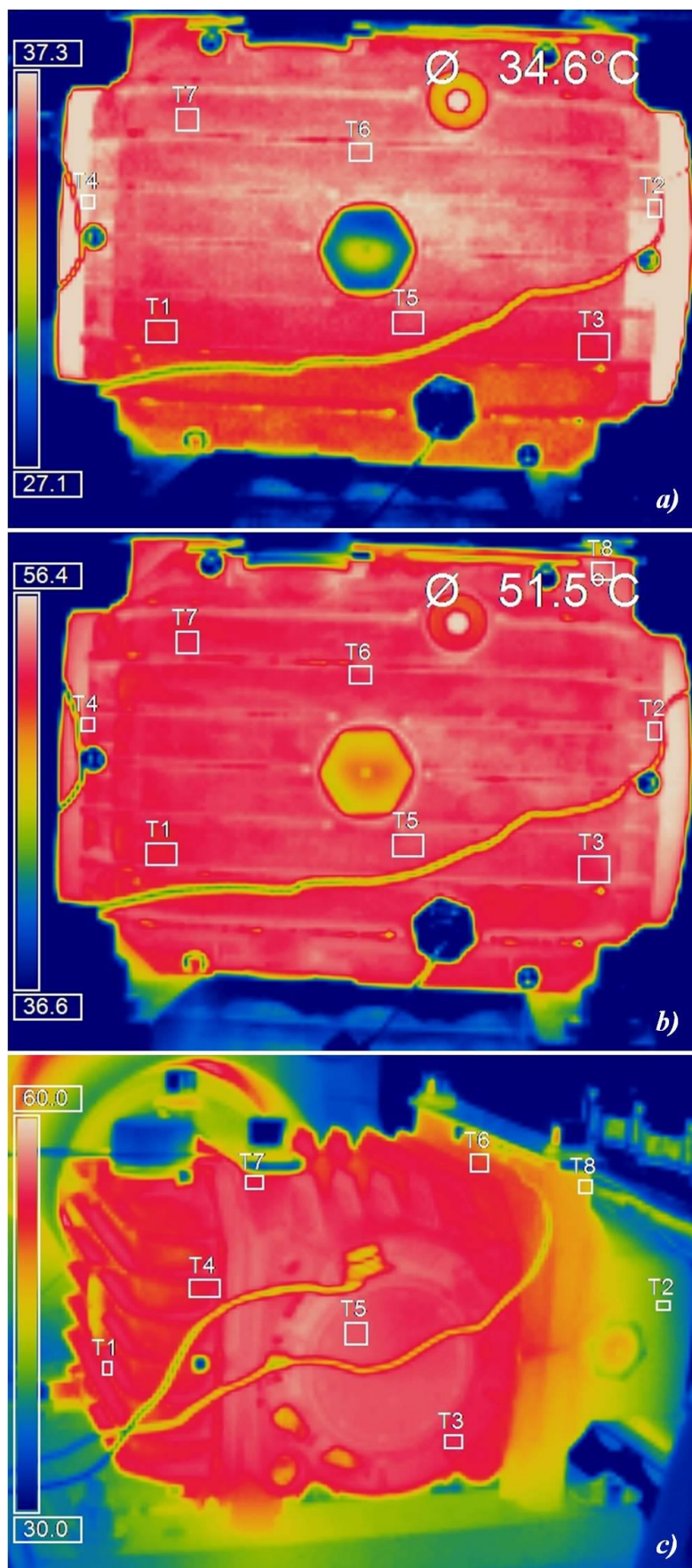
Figs. 4. Pumping side analysis: a) Phasing of piston chamber volume; b) load flow rate; c) load pressure

Once the pumping side is tailored and validated, the mechanical side of the pump model can be completed. In particular, the heat transfer coefficient and the air-oil distribution of each surface of the internal geometry of the crankcase are achieved from the 2D CFD model and they are employed in the lumped parameter model in order to enhance the accuracy.

The validation of the whole pump model is achieved comparing the numerical results with the measurements carried out by means of thermocouples type K, placed in different positions of the crankcase, on the external walls and in the internal oil volume. The experimental oil temperature curve has been obtained as a mean of the measurements carried out and it has been used to tailor the numerical model. Water and air temperature are monitored, and the ambient temperature is recorded too. Both transient and steady-state operations are considered.

Afterwards, a thermographic camera is adopted in order to obtain a complete temperature distribution of the external walls of the machine. The device used is a Optris PI 600 thermocamera characterized by a spectral range of 7.5-1.3 μm , a temperature range from -20°C to 900°C and an optical resolution of 160×120 pixel; the frequency is 120 Hz.

Fig. 5 shows the thermal images in different positions: the temperature reported at the top of each image (e.g., 34.6°C in Fig. 4a) is relative to the average value of all the pixel that compose the T1 probe box. In the case shown in Figs. 5a and 5b, the camera is positioned in front of the crankcase cover, the opposite part of the pump cylinder head side. By monitoring the heating transient, it is possible to observe how the hottest parts, the needle bearings and the shaft, progressively transfer thermal power from the middle plane to the upper and the lower side, until the wall is almost at the same temperature (in steady-state condition, see Fig. 5b). This consideration about the uniformity of the temperature confirms that the lumped parameter approach can be used to describe the system with a good accuracy: indeed, if the temperature distribution on each component is uniform, the error due to the description of each part as an numerical element characterized by a single temperature value, is very limited. Fig. 5c shows the whole crankcase from a different view in the steady state condition: in particular, the cooling effect of the pump cylinder head (where the water flows) can be observed on the left side. The effect is restricted to a narrow zone but it can not be neglected: for this reason, the lumped and distributed parameter model is referred to the whole pump and it account for both thermal power dissipation between the crankcase and the environment and between the crankcase and the pump cylinder head.



Figs. 5. Thermographic analysis: a) crankcase cover after a few seconds; b) crankcase cover in steady-state condition; c) whole pump in steady-state condition

As mentioned above, the experimental campaign is carried out to tailor and validate the numerical model of the pump. Fig. 6 shows the comparison between the measured oil temperature and the numerical one, as well as the numerical air temperature. More in details, the model can not consider a multiphase fluid; thus, two separated fluids are included and so, two numerical temperatures are obtained. Each phase is able to exchange thermal power with the surfaces which are in contact, on the basis of the air/oil distribution obtained from the 2D CFD model. Two volumes are used, one for the air and the other one for the oil. Each volume is equal to the 50% of the internal volume of the crankcase. Nevertheless, in Fig. 6 it is possible to observe that the two numerical temperatures are perfectly overlapped, as a consequence of the model reliability. In fact, even if air and oil have no direct interfaces in the model, they are in contact with the same surfaces and it seems physically correct that the two curves are equal. In particular, due to the strongly different thermo physical properties of the two fluids, the thermal equilibrium is mainly influenced by the oil. Thus, the comparison is based on the oil temperature: the agreement is excellent for the steady-state condition (the error is around the 2%) but the numerical curve increases faster than the experimental one in the transient phase. This is due, on the one hand, to the 3D effect of the heat transfer phenomenon, that the lumped model can not consider, and on the other hand, to the employed data logger. In fact, in order to remove the noise from the signal, the data logger automatically applies a moving average to the raw data. This increases the quality of the signal, but it introduces a delay. Both the 3D effect and the signal treatment influence are more significant during the transient phase than the steady-state phase. In order to enhance the lifetime of the pump, it is very important to avoid too high temperature when the machine operates continuously; thus, it is possible to accept a quite poor agreement between numerical and experimental data in the transient phase because, in the steady state condition, the agreement is very good. The overheating risk regards only the mechanical side of the pump. In fact, observing Figs. 4 and 6, the hydraulic transient of the pumping side is strongly minor than the thermal transient of the mechanical side: after a few seconds, the load flow rate and pressure are in steady state condition, while the oil temperature of the lubricating system requires more than 4000 s to be stable. Thus, the lubricating system temperature does not influence directly the operating point of the pump: the pumping side temperature is fixed by the water flow.

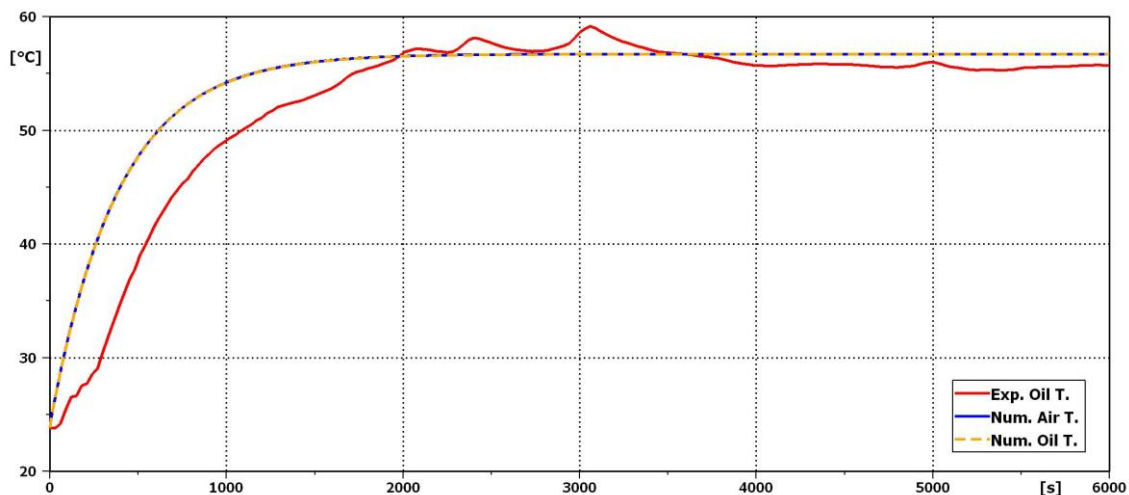


Figure 6. Comparison between measured and calculated oil temperature

6. CONCLUSIONS

This paper has presented a numerical approach for the prediction of the thermo fluid dynamics behaviour of a piston water pump. Particular care has been devoted to the lubricating system model and to the heat transferred from the internal crankcase to the environment. A 2D CFD model of the system has been constructed, accounting for the thermal power released by friction, the mixing of the two fluids (oil and air) in the crankcase volume, the moving parts (rod and piston) described by means of the overset mesh technique.

The outputs of the 2D CFD model, in terms of heat transfer coefficient and air/oil distribution of each surfaces, have been passed to a lumped and distributed parameter model of the whole pump, properly designed to describe both the operating point of the pumping side and the thermal condition of the mechanical side. Conduction and convection phenomena between the pump cylinder head and the crankcase, and between the crankcase and the environment have been included. The model has been tailored and validated using experimental data carried out by means of two different measurements technique: thermocouples analysis and thermography. The employed thermocamera has highlighted that the temperature of each component has a uniform distribution, confirming the most important hypothesis for the use of the lumped parameter approach.

The numerical results, in terms of oil temperature, have been compared with the acquired data and a good agreement has been found, especially in the steady-state condition. Simulation and measurements have confirmed that the water flow has a cooling effect on the pumping side and the temperature in this zone is fixed by the water. In fact, the operating point of the pump is not influenced by the thermal transient of the lubricating system. On the other hand, even if the crankcase is partially cooled by the conduction between the component itself and the pump cylinder head, this phenomenon is not sufficient to maintain the mechanical side temperature under the overheating limit without adopting a lubricating system.

Combing the 2D CFD lubricating system model and the lumped parameter model of the whole pump, the user can achieve all the information needed to properly design the machine and in particular the lubricating system. The approach is able to ensure a good accuracy in an acceptable time: both the operating point and the thermo fluid dynamics behaviour of the pump are described and the computational effort is minor than the one referred to a complete 3D CFD model.

AKNOWLEDGEMENT

The Authors would like to acknowledge Dr. Davide Bottazzi for the important contribution to this work for both the experimental analysis and the simulation approach.

632 LIST OF NOTATIONS

a	Thermal diffusivity	m^2/s
Ar	Cross section area	m^2
b	Volumetric thermal expansion coefficient	K^{-1}
\bar{c}	Mean radial clearance	m
C	Coefficient	-
C_0	First coefficient of k_{oil} correlation	$0.053\text{W}/(\text{m}^*\text{K})$
C_1	Second coefficient of k_{oil} correlation	$0.026\text{W}/(\text{m}^*\text{K})$
C_2	First coefficient of c_{poil} correlation	$1.17*10^6\text{J}/(\text{m}^3*\text{K})$
C_3	Second coefficient of c_{poil} correlation	$0.39*10^6\text{J}/(\text{m}^3*\text{K})$
c_p	Specific heat	$\text{J}/(\text{kg}*\text{K})$
d	Diameter	m
F	Force	N
g	Gravitational constant	m/s^2
Gr	Grashof number	-
h	Heat transfer coefficient	$\text{W}/(\text{m}^2*\text{K})$
k	Thermal conductivity	$\text{W}/(\text{m}^*\text{K})$
l	Length	m
M	Torque	$\text{N}*\text{m}$
n	Number of	-
nc	Convection exponent	-
nd	Coefficient of covered area	-
Nu	Nusselt number	-
p	Pressure	Pa
P	Power	W
Per	Perimeter	m
Pr	Prandtl number	-
Q	Flow rate	m^3/s
r	Radius	m
R	Thermal resistance between the internal and the external case wall	$\text{K}*\text{m}^2/\text{W}$
Ra	Rayleigh number	-

Re	Reynolds number	-
R_g	Perfect gas law constant	J/(mol*K)
s	Wall thickness	m
S	Surface area	m ²
t	Time	s
T	Temperature	K
v	Velocity	m/s
V	Volume	m ³
W_{cond}	Thermal power transferred through the wall	W
W_{conv}	Thermal power transferred between the wall and the environment	W
y	Position referred to the Y axis	m
\dot{y}	Velocity referred to the Y axis	m/s
x	Position referred to the X axis	m
\dot{x}	Velocity referred to the X axis	m/s
α	Angle between crank and piston axis	rad
β	Angle between rod and piston axis	rad
$\dot{\beta}$	Rod rotational speed	rad/s
η	Efficiency	-
λ	Ratio between crank and rod length	-
ρ	Density	Kg/m ³
μ	Dynamic viscosity	Pa*s
ω	Crankshaft rotational speed	rad/s

633 Subscripts

A	Point A - connecting rod small end
air	Air
B	Point B - connecting rod big end
c	Crank
cer	Ceramic
eff	Effective
env	Environment
ext	External
geo	Geometrical
f	Friction

<i>h</i>	hydraulic
<i>head</i>	Pump cylinder head
<i>hm</i>	Hydro-mechanical
<i>hyd</i>	Hydraulic
<i>int</i>	Internal
<i>jb</i>	Journal box
<i>J</i>	Point J – generic rod point
<i>max</i>	Maximum value
<i>mech</i>	Mechanical
<i>nb</i>	Needle bearing
<i>oil</i>	Oil
<i>p</i>	Piston
<i>r</i>	Connecting rod
<i>ref</i>	Reference value
<i>ring</i>	Seal placed in the cylinder wall
<i>rbe</i>	Rod big end
<i>rse</i>	Rod small end
<i>suc</i>	Suction
<i>sh</i>	Shaft
<i>tot</i>	Total
<i>vol</i>	Volumetric
<i>wall</i>	Crankcase wall
<i>water</i>	Water

634

635 REFERENCES

- 636 [1] M.M.A. Bhutta, N. Hayat, M.H. Bashir, A.R. Khan, K.N. Ahmad, S. Khan, CFD
637 applications in various heat exchangers design: A review, Appl. Therm. Eng. 32
638 (2012) 1-12.
- 639 [2] H. Mroue, J.B. Ramos, L.C. Wrobel, H. Jouhara, Performance evaluation of a
640 multi-pass air-to-water thermosyphon-based heat exchanger, Energy 139 (2017)
641 1243-1260, <http://dx.doi.org/10.1016/j.energy.2017.04.111>.
- 642 [3] Valentin Guichet , Hussam Jouhara , Condensation, evaporation and boiling of
643 falling films in wickless heat pipes (two-phase closed thermosyphons): a critical
644 review of correlations, International Journal of Thermofluids (2019), doi:
645 <https://doi.org/10.1016/j.ijft.2019.100001>
- 646 [4] S.R. Shah, S.V. Jain, R.N. Patel, V.J. Lakhera, CFD for centrifugal pumps: a review
647 of the state-of-the-art, Procedia Eng. 51 (2013) 715–720.
- 648 [5] J.B. Heywood, Internal Combustion Engine Fundamentals, 1st ed., McGraw-Hill,
649 Inc., New York, 1988.

- 650 [6] J.R. Cho, S.J. Moon, A numerical analysis of the interaction between the piston oil
651 film and the component deformation in a reciprocating compressor, *Tribol. Int.* 38
652 (2005) 459–468.
- 653 [7] A. Menéndez Blanco, J.M. Fernández Oro, Unsteady numerical simulation of an
654 air-operated piston pump for lubricating greases using dynamic meshes, *Comput.*
655 *Fluids* 57 (2012) 138–150.
- 656 [8] G.A. Livanos, N.P. Kyrtatos, Friction model of a marine diesel engine piston
657 assembly, *Tribol. Int.* 40 (2007) 1441–1453.
- 658 [9] Y. Tateishi, Tribological issues in reducing piston ring friction losses, *Tribol. Int.*
659 27 (1994) 17–23.
- 660 [10] S.K. Chen, P. Flynn, Development of a compression ignition research engine, No.
661 650733, SAE Paper (1965).
- 662 [11] P.R. Hooper, T. Al-Shemmeri, M.J. Goodwin, An experimental and analytical
663 investigation of a multi-fuel stepped piston engine. *Appl. Therm. Eng.* 48 (2012)
664 32–40.
- 665 [12] Hussam Jouhara, Bandar Fadhl, Luiz C. Wrobel, Three-dimensional CFD
666 simulation of geyser boiling in a two-phase closed thermosyphon, *international*
667 *journal of hydrogen energy* 41 (2016) 16463–16476,
668 <http://dx.doi.org/10.1016/j.ijhydene.2016.02.038>
- 669 [13] A.J. Lückmann, M.V.C. Alves, J.R. Barbosa Jr., Analysis of oil pumping in a
670 reciprocating compressor, *Appl. Therm. Eng.* 29 (2009) 3118–3123.
- 671 [14] Andrea Bassi, Massimo Milani, Luca Montorsi, Stefano Terzi, Dynamic Analysis
672 of the Lubrication in a Wet Clutch of a Hydromechanical Variable Transmission,
673 SAE Int. Journal of Commercial Vehicles, Volume 9 (2016).
- 674 [15] Terzi, S., Manhartgruber, B., Milani, M., and Montorsi, L., “Optimization of the
675 Lubrication Distribution in Multi Plate Wet-Clutches for HVT Transmissions: An
676 Experimental - Numerical Approach,” SAE Technical Paper 2018-01-1822, 2018,
677 doi:10.4271/2018-01-1822.
- 678
- 679 [16] W. Habchi, P. Vergne, S. Bair, O. Andersson, D. Eyheramendy, G.E. Morales-
680 Espejel, Influence of pressure and temperature dependence of thermal properties of
681 a lubricant on the behaviour of circular TEHD contacts, *Tribol. Int.* 43 (2010) 1842–
682 1850.
- 683 [17] C.D. Rakopoulos, G.M. Kosmadakis, E.G. Pariotis, Critical evaluation of current
684 heat transfer models used in CFD in-cylinder engine simulations and establishment
685 of a comprehensive wall-function formulation, *Appl. Energy* 87 (2010) 1612–1630.
- 686 [18] F.P. Incropera, D.P. DeWitt, Fundamentals and heat and mass transfer, 5th ed.,
687 John Wiley and sons, New York, 2002.
- 688 [19] W.H. McAdams, Heat transmission, McGraw-Hill, New York, 1954.
- 689 [20] K.A. Brucker, J. Majdalani, Effective thermal conductivity of common geometric
690 shapes, *Int. J. Heat Mass Transf.* 48 (2005) 4779–4796.
- 691 [21] A.W. Churchill, H.H.S. Chu, Correlating equations for laminar and turbulent free
692 convection from a vertical plate, *Int. J. Heat Mass Transf.* 18 (1975) 1323–1329.

[22] D. Bottazzi, S. Farina, M. Milani, L. Montorsi, A numerical approach for the analysis of the coffee roasting process, J. Food Eng. 112, Issue 3, (2012) 243–252.

APPENDIX A

$$\alpha = \omega \cdot t \quad (\text{A.1})$$

$$\sin \beta = (r_c / l_r) \cdot \sin \alpha = \lambda \cdot \sin \alpha \quad (\text{A.2})$$

$$\sin^2 \beta = \lambda^2 \cdot \sin^2 \alpha \quad (\text{A.3})$$

$$\sin^2 \beta + \cos^2 \beta = \lambda^2 \cdot \sin^2 \alpha + \cos^2 \beta \quad (\text{A.4})$$

$$\cos \beta = \sqrt{1 - \lambda^2 \cdot \sin^2 \alpha} \quad (\text{A.5})$$

$$x = (r_c + l_r) - r_c \cdot \cos \alpha - l_r \cdot \cos \beta = r_c \left[(1 + 1/\lambda) - \cos \alpha - (1/\lambda) \cdot \sqrt{1 - \lambda^2 \cdot \sin^2 \alpha} \right] \quad (\text{A.6})$$

$$\dot{x} = \frac{dx}{dt} = \frac{dx}{d\alpha} \cdot \frac{d\alpha}{dt} = r_c \cdot \omega \cdot \left[\sin \alpha + \frac{\lambda \cdot \sin \alpha \cdot \cos \alpha}{\sqrt{1 - \lambda^2 \cdot \sin^2 \alpha}} \right] = r_c \cdot \omega \cdot \left[\sin \alpha + \frac{\lambda \cdot \sin 2\alpha}{2 \cdot \sqrt{1 - \lambda^2 \cdot \sin^2 \alpha}} \right] \quad (7)$$

$$\beta = \arcsin(\lambda \cdot \sin \alpha) \quad (\text{A.7})$$

$$\frac{d\beta}{dt} = \frac{1}{\sqrt{1 - \lambda^2 \cdot \sin^2 \alpha}} \cdot \lambda \cdot \cos \alpha = \lambda \cdot \frac{\cos \alpha}{\cos \beta} \quad (\text{A.8})$$

$$\dot{\beta} = \frac{d\beta}{dt} = \frac{d\beta}{d\alpha} \cdot \frac{d\alpha}{dt} = \lambda \cdot \omega \cdot \frac{\cos \alpha}{\cos \beta} = \lambda \cdot \omega \cdot \frac{\cos \alpha}{\sqrt{1 - \lambda^2 \cdot \sin^2 \alpha}} \quad (6)$$

APPENDIX B

$$\text{Re}_{\text{wall_ext}} = (v_{\text{env}} \cdot \rho_{\text{env}} \cdot l_{\text{wall_ext}}) / \mu_{\text{env}} \quad (\text{B.1})$$

$$\text{Pr}_{\text{env}} = \mu_{\text{env}} / (\rho_{\text{env}} \cdot a_{\text{env}}) \quad (\text{B.2})$$

$$\text{Gr}_{\text{wall_ext}} = g \cdot b_{\text{env}} \cdot (T_{\text{wall_ext}} - T_{\text{env}}) \cdot l_{\text{wall_ext}} \cdot \rho_{\text{env}} / \mu_{\text{env}} \quad (\text{B.3})$$

$$\text{Ra}_{\text{wall_ext}} = \text{Pr}_{\text{env}} \cdot \text{Gr}_{\text{wall_ext}} \quad (\text{B.4})$$

$$d_h = 4 \cdot Ar / \text{Per} \quad (\text{B.5})$$

$$\text{Re}_{\text{sh_oil}} = (\omega \cdot \rho_{\text{oil}} \cdot d_{\text{sh}}) / \mu_{\text{oil}} \quad (\text{B.6})$$